HETEROCYCLES, Vol. 102, No. 7, 2021, pp. 1301 - 1313. © 2021 The Japan Institute of Heterocyclic Chemistry
Received, 17th February, 2021, Accepted, 23rd April, 2021, Published online, 20th May, 2021
DOI: 10.3987/COM-21-14432

UNCOMMON REACTIVITY OF A *SECO*-OXACASSANE DITERPENOID AND ANTIPROLIFERATIVE ACTIVITY OF SOME DERIVATIVES

Alexia Hernández-Jiménez,[a] Ledy De-la-Cruz-Martínez,[a] Raúl Velasco-Azorsa,[a] Reyna Zeferino-Díaz,[a] José G. Alvarado-Rodríguez,[a] Luis H. Mendoza-Huizar,[a] J. Jesús Manríquez-Torres,[b] Horacio Almanza-Reyes,[b] Carlos M. Cerda-García-Rojas,[c] Pedro Joseph-Nathan,[c] and J. Martín Torres-Valencia[a]*

[a]Área Académica de Química, Universidad Autónoma del Estado de Hidalgo, km 4.5 Carretera Pachuca-Tulancingo, Mineral de la Reforma, Hidalgo 42184, México; [b]Escuela de Medicina y Psicología, Universidad Autónoma de Baja California, Tijuana, Baja California 22390, México; [c]Departamento de Química, Centro de Investigación y de Estudios Avanzados del Instituto Politécnico Nacional, Apartado 14-740, México City 07000, México. E-mail: jmartin@uaeh.edu.mx

Abstract – The main diterpenoid of *Acacia schaffneri*, 7,8-*seco*-7,8-oxacassa-13,15-dien-7-ol-17-al (**1**), has two aldehydes of which one is protected as a *ε*-lactol. The free aldehyde resisted to afford the carboxylic acid using reagents with different oxidative strength, although **1** gave oxime **2** when treated with hydroxylamine, *β*-hydroxyketone **3** after addition of acetone, aldo-*ε*-lactone **4** whereby only the lactol was oxidized when using Jones reagent, and epoxyformate **5** after Baeyer-Villiger treatment. Hydrolysis of **5** with $NaHCO_3$ gave **6**. Structures **2**–**6** followed from physical and spectral data including X-ray diffraction. All compounds showed antiproliferative activity similar to some chemotherapeutic drugs against C2C12, L929, SiHa, and MDA-MB-231 cell lines.

INTRODUCTION

The quite uncommon chemical structure of the main diterpenoid isolated from the aerial parts of *Acacia schaffneri*,[1] 7,8-*seco*-7,8-oxacassa-13,15-dien-7-ol-17-al (**1**) (Scheme 1), makes it attractive to search for cytotoxic activity based on the general idea that naturally occurring products with rare atom arrangements might possess unexpected biological properties. This reasoning is in line with the fact that during the last decades many anticancer treatments were developed using naturally occurring substances as the starting

point for the preparation of new active products[2] since secondary metabolites and their chemical derivatives are recognized as an unlimited source for the discovery of new biocompatible therapeutic agents.[3] Furthermore, it was quite recently evidenced that a closely related naturally occurring vouacapane diterpenoid and several of its derivatives turned out to be cytotoxic.[4] In addition, a preliminary study revealed that **1** possesses some cytotoxic activity. This effect against colon HT-29, lung A-549, and skin cancer UACC-62 cell lines is comparable with that of the drug 5-fluorouracil, although little selectivity was observed when its cytotoxicity was evaluated against healthy cell counterparts.[5] The mechanism of action of **1** was suggested as a DNA alkylating agent, in which the *γ*,*δ*-unsaturated carbonyl system is important for the activity and can act as an extended Michael acceptor.[5] Since, in addition to the unsaturated aldehyde system, **1** possesses another aldehyde group which is protected as a seven member ring hemiacetal, the molecule is a good candidate for structure modifications. Thus, nucleophilic additions and oxidation reactions were performed to generate and search for new cytotoxic agents. Therefore, in this work five new derivatives of **1** were prepared, including oxime **2**, *β*-hydroxyketone **3**, aldo-*ε*-lactone **4**, epoxyformate **5**, and 17-*nor*-ketone **6** (Scheme 1). The new compounds, containing an oxepane ring, were characterized by physical and spectroscopic means including HRESIMS, ^{1}H and ^{13}C NMR measurements. The structures were further verified by single-crystal X-ray diffraction analyses which allowed defining some stereochemical aspects. Of relevance is to mention that the aldehyde group of **1** was resistant to oxidation to afford the corresponding carboxylic acid, a behavior that seems unprecedented for an aldehyde group. The evaluation of the antiproliferative activity of **1**–**6** against mouse muscle myoblast C2C12, mouse fibroblast L929, human cervical carcinoma SiHa, and human breast adenocarcinoma MDA-MB-231 cell lines was undertaken.

RESULTS AND DISCUSSION

Diterpenoid **1** was obtained in adequate amounts for the preparation of **2**–**6** from the aerial parts of *A. schaffneri*.[1] Nucleophilic addition of hydroxylamine to **1** gave **2** in 66% yield, while aldol condensation of **1** with acetone in basic medium led to *β*-hydroxyketone **3** in 43% yield. The corresponding ^{1}H NMR spectra did not evidence both *syn* and *anti* oximes for **2**, nor the absolute configuration (AC) of C-17 in the case of **3**. However, the *anti* oxime geometry in **2** and the (17*S*) AC in **3** followed from the X-ray diffraction (XRD) studies detailed below. Although **3** was not the only expected condensation product, the *γ*,*δ*-unsaturated carbonyl compound could not be obtained even when using large excesses of acetone and NaOH.

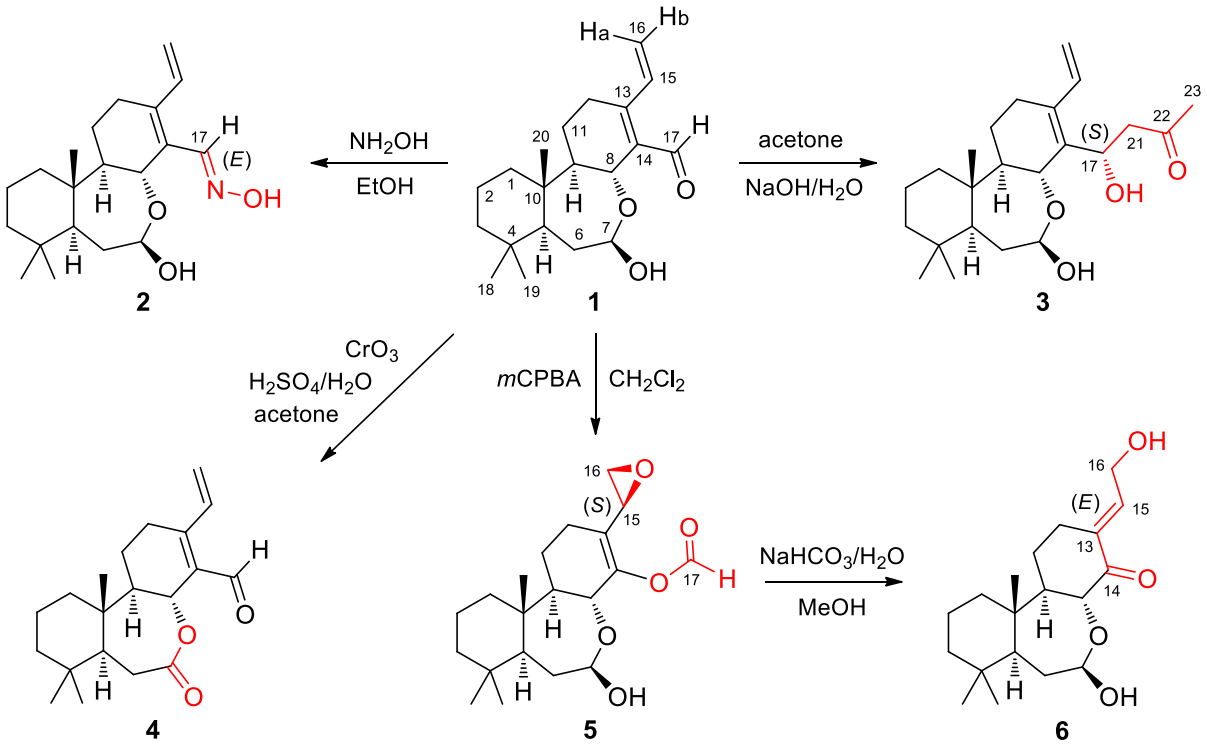

Scheme 1. Preparation of *seco*-oxacassane derivatives **2**–**6** starting from natural diterpenoid **1**

Due to the appropriate reactivity of the aldehyde group in the two previous reactions, and considering that the solubility of the diterpenoid in protic media, for cytotoxic studies, would improve after oxidizing the aldehyde to the corresponding carboxylic acid, and that such a reaction might be selective under mild reaction conditions, compound **1** was treated with Ag_2O in the presence of NH_4OH using Tollens reaction conditions, a task, that to our surprise, was unsuccessful since the starting aldehyde **1** was recovered. This result seems unprecedented as the beautiful silver mirror in the bottom of a test tube,[6] after a Tollens spot test, was considered infallible and consequently the structure elucidation of **1**, before the advent of ^{1}H NMR some 60 years, would have been extremely difficult. Attempts to obtain the C-17 carboxylic acid were unsuccessful when **1** was treated with aqueous $K_2Cr_2O_7/H_2SO_4$, $NaClO_2$,[7] CuCl/*t*-BuOOH,[8] hypervalent iodine reagent 1-hydroxy-1,2-benziodoxol-3(1*H*)-one 1-oxide (IBX),[9] or Mohr salt/$(NH_4)_2Fe(SO_4)_2$•$6H_2O$]/*t*-BuOOH.[10] In most cases, aldehyde **1** remained unchanged and, in the treatment with $K_2Cr_2O_7/H_2SO_4$, an intractable mixture of products was obtained.

The reluctance of the aldehyde group for oxidation even in the presence of a strong oxidizing agent became evident when treatment of **1** with Jones reagent[11] cleanly gave the aldo-ε-lactone **4** in high yields (83%) wherein the C-7 hemiacetal was transformed into the lactone group, while the aldehyde group remained untouched. In contrast, Baeyer-Villiger oxidation[12] of **1** using *m*-chloroperbenzoic acid induced two chemical changes, the formations of the C-15–C-16 epoxide and the C-14 formate to provide **5** in 59% yield and 64% of diastereoselectivity towards the (15*S*)-stereoisomer, as evidenced by a combination of ^{1}H

NMR and XRD, since both epimers at C-15 were formed but only one of them provided crystals suitable for an XRD study. Finally, alkaline treatment of **5** with aqueous $NaHCO_3$ led to 17-*nor*-ketone **6** in 68% yield. Both (15*S*)- and (15*R*)-stereoisomers of **5** are converted into a single product through keto-enol tautomerism of the intermediate enolate, which arises after hydrolysis of the formate group, generating the C-14 ketone, which also induces the double bond migration from C-13–C-14 to C-13–C-15 with concomitant epoxide opening to afford the C-16 primary alcohol.

Compounds **2**–**6** were characterized by ^{1}H and ^{13}C NMR measurements (Tables 1 and 2, respectively) with the aid of gCOSY, gHSQC, and gHMBC experiments, as well as by comparison with the data of **1**.[1] The ^{1}H NMR spectrum of **2** showed the oxime H-17 singlet at δ_H 8.33 and two broad signals at δ_H 10.68 and 7.55 owing to the hydroxy groups of the oxime and the H-7 hemiacetal, respectively. The signals due to the vinyl H-15, H-16a, and H-16b atoms were observed at δ_H 6.85 (dd, J = 17.2, 11 Hz), 5.43 (d, J = 17.2 Hz), and 5.32 (d, J = 11.0 Hz), respectively, while H-7 and H-8 appeared at δ_H 5.14 (dd, J = 8.5 and 6.7 Hz) and 4.82 (d, J = 8.9 Hz), respectively. The ^{13}C NMR spectrum of **2** showed the C-17 oxime carbon at δ_C 149.9, which was assigned using its gHSQC correlation with H-17, while the remaining signals resembled those of **1**.

The ^{1}H NMR spectrum of **3** showed the characteristic signals of the terminal double bond at δ_H 6.57 (dd, J = 17.2, 11.0 Hz, H-15), 5.25 (d, J = 17.2 Hz, H-16a), and 5.13 (d, J = 11.0 Hz, H-16b), a broad doublet at δ_H 5.30 (J = 10.7 Hz) for H-17 which is geminal to a hydroxy group, and signals for the acetone residue at δ_H 3.39 (dd, J = 17.3, 10.7 Hz, H-21), 2.65 (dd, J = 17.3, 2.4 Hz, H-21') including the Me-23 methyl ketone singlet at δ_H 2.21. COSY correlations of the H-17 signal (δ_H 5.30) with the methylene protons at C-21 (δ_C 52.2) were observed. In the ^{13}C NMR spectrum of **3**, four vinyl carbon signals were observed at δ_C 136.1 (C-13), 133.8 (C-14), 133.0 (C-15), and 115.4 (C-16). The signal for the carbon atom bearing the hydroxy group (C-17) was observed at δ_C 67.2, while the signals due to the acetone residue were observed at δ_C 210.4 (C-22), 52.2 (C-21), and 30.4 (C-23). The gHMBC experiment of **3** showed the correlation between the signals of H-21 and Me-23 with the carbonyl carbon signal at δ_C 210.4.

The ^{1}H NMR spectrum of aldo-ε-lactone **4** displayed a singlet at δ_H 10.19 for the H-17 aldehyde and signals at δ_H 7.27 (dd, J = 17.2, 11.0 Hz, H-15), 5.67 (d, J = 17.2 Hz, H-16a), and 5.59 (d, J = 11.0 Hz, H-16b) for the γ,δ-unsaturated carbonyl system. Also, a broad doublet (J = 7.8 Hz) was observed for H-8 at δ_H 5.52 geminal to the lactone moiety.

In the spectrum of **4**, the H-7 hemiacetal signal was absent in comparison with the ^{1}H NMR spectrum of **1**, while the H-6α and H-6β signals were shifted to higher frequencies and now appear at δ_H 2.50 (d, J = 14.2 Hz) and 2.86 (dd, J = 14.2, 10.4 Hz), respectively, since they are alpha to a carbonyl group. The ^{13}C NMR spectrum of **4** displayed signals at δ_C 189.2 and 176.0 for the C-17 aldehyde and the C-7 lactone carbonyl

groups, respectively. The double bond carbons conjugated with the aldehyde group showed similar chemical shifts as those of **1**, while the C-8 signal, bearing the lactone group, appeared at δ_C 72.1. In addition, the gHMBC experiment of **4** showed correlation of H-8 and the carbonyl group signals.

The ^{1}H NMR spectrum of **5** exhibited the H-17 formate singlet at δ_H 8.11, while the epoxide group signals appeared at δ_H 3.62 (dd, J = 4.4, 2.7 Hz, H-15), 2.88 (dd, J = 5.2, 4.4 Hz, H-16a), and 2.73 (dd, J = 5.2, 2.7 Hz, H-16b). The COSY experiment showed correlations between H-15 and H-16a and H-16b, as well as between the last two protons. The ^{13}C NMR spectrum of **5** presented signals at δ_C 160.6 due to the carbonyl carbon of the formate group (C-17), and at δ_C 48.0 (C-15) and 45.5 (C-16) for the epoxide group carbon atoms. The signals of the vinyl carbons were appreciated at δ_C 146.0 (C-14) and 127.3 (C-13), whose distinction was achieved based on the gHMBC experiment, in which the correlation between the H-17 and the δ_C 146.0 signal was evident.

The ^{1}H NMR spectrum of **6** displayed a triplet (J = 5.6 Hz) at δ_H 6.62 for the H-15 vinyl atom, two double doublets at δ_H 4.32 and 4.27 (J = 15.2, 5.6 Hz) for the methylene hydrogen atoms at C-16 bearing the hydroxyl group, and two signals at δ_H 5.13 (dd, J = 9.2, 5.0 Hz) and 4.22 (d, J = 11.1 Hz) for H-7 and H-8, respectively. Its ^{13}C NMR spectrum showed 19 signals, including those at δ_C 200.5 for the carbonyl carbon (C-14), 136.9 and 136.8 due to the C-15 and C-13 vinyl carbons, respectively, and the C-16 signal at δ_C 59.5 for the hydroxy group bearing carbon. The C-7 hemiacetal carbon signal and the C-8 oxygen bearing carbon atom were observed at δ_C 95.6 and 74.6, correspondingly, while the C-14 ketone group was corroborated by a gHMBC experiment which showed the correlation of H-8 and the carbonyl group signal.

Samples of **2**–**6** were further evaluated by single-crystal X-ray diffraction studies which provided independent structural proof and evidenced some stereochemical details. The relevant crystal data, showing that XRD structure determinations could be performed in all cases, can be inspected in Table 3 which includes the results of Flack[13] and Hooft[14] parameters calculations thereby demonstrating the absolute configuration of the molecules. PLUTO plots for **2**–**6** are depicted in Figure 1. These studies also confirmed the *anti* oxime formation in **2** and the (17*S*) AC in the case of **3**. Likewise, the (15*S*)-epoxide in **5** is evidenced in the corresponding PLUTO plot derived from the crystals. The compound was obtained as a mixture of C-15 epimers as judged by ^{1}H NMR measurements and addition of a precise amount of the crystals to the mixture was done to verify which was the predominant epimer. Finally, the (*E*)-$\Delta^{13(15)}$ double bond and the C-14 carbonyl carbon in 17-*nor*-ketone **6** were conclusively supported by the XRD study.

Compounds **1**–**6** were evaluated against C2C12, L929, SiHa, and MDA-MB-231 cell lines using the MTT assay[15] for 24 and 48 h as summarized in Table 4. All compounds showed relevant activity providing an IC_{50} range between 0.05 and 2.95 μM, with the highest activity occurring after 48 h. Compound **5** showed

the best value IC_{50} (0.05 μM) against L929 after 48 h, while **6** presented the highest value (2.95 μM) against SiHa after 24 h. Diterpenoid **1** displayed IC_{50} values between 0.11 and 1.08 μM for the studied cells and showed remarkable activity against SiHa (0.11 μM). Other molecules showed activity variations as can be observed in the tabulated data. For instance, **2** presented strong growth inhibition of the four cell lines, while in the case of **3** the best activity was against MDA-MB-231 cell line (IC_{50} = 0.34 μM). In turn, **4** exhibited its best activity against L929 (IC_{50} = 0.22 μM). In comparison with standard chemotherapeutic drugs, such as 5-fluorouracil (5-FU) (IC_{50} = 2.98 μM against L929,[16] and 11.40 μM against MDA-MB-231[17]), and cisplatin (IC_{50} = 7.84 μM against SiHa, and 19.13 μM against MDA-MB-231),[18] the studied compounds seem to be of relevance for their antiproliferative activity.

Table 1. ^{1}H NMR Data for **2**–**6** in $CDCl_3$ at 400 MHz

	δ_H, mult. (*J* in Hz)				
Position	**2**[a]	**3**[b]	**4**	**5**[c]	**6**[d]
1α	1.01, td (13.0, 3.8)	0.97, td (13.0, 3.0)	1.04, td (12.8, 3.2)	0.98, td (13.2, 3.7)	1.04, td (13.5, 3.4)
1β	1.96, dq (13.0, 1.5)	1.96, dq (13.0, 2.3)	1.82, dtd (12.8, 3.2, 1.6)	1.92, br d (13.2)	1.91, m
2α	1.54, dt (13.5, 2.9)	1.53, dt (13.6, 2.7)	1.59, m	1.51, br d (12.0)	1.60, m
2β	1.47, m	1.45, m	1.54, m	1.43, m	1.46, m
3α	1.16, td (13.4, 4.2)	1.82, br t (13.8)	1.22, td (13.8, 4.7)	1.15, td (13.0, 4.2)	1.17, td (13.2, 2.9)
3β	1.44, m	1.44, m	1.48, dtd (13.8, 3.2, 1.6)	1.42, m	1.43, m
5	1.27, dd (7.2, 2.6)	1.23, dd (9.3, 4.9)	1.42, d (10.4)	1.28, d (8.3)	1.30, d (9.2)
6α	1.89, m	1.86, m	2.50, d (14.2)	1.86. m	1.88, m
6β	1.88, m	1.85, m	2.86, dd (14.2, 10.4)	1.70, m	1.65, m
7	5.14, dd (8.5, 6.7)	5.10, t (7.7)	—	5.09, ddd (9.4, 5.0, 3.5)	5.13, dd (9.2, 5.0)
8	4.82, d (8.9)	4.83, br d (8.3)	5.52, br d (7.8)	4.51, dd (10.4, 2.0)	4.22, d (11.1)
9	1.35, ddd (13.0, 9.8, 2.1)	1.25, m	1.58, m	1.37, ddd (13.0, 9.1, 2.1)	1.57, m
11α	1.88, m	1.83, m	1.96, dq (13.0, 3.5)	1.82, m	1.91, m
11β	1.08, td (13.0, 4.1)	1.09, qd (12.4, 4.2)	1.13, dddd (13.7, 13.2, 12.4, 3.8)	1.23, br d (13.2)	1.34, m
12α	2.16, br dd (18.0, 14.8)	2.06, ddd (16.7, 15.6, 3.0)	2.26, ddd (18.0, 13.7, 3.1)	1.84, m	2.21, br dd (16.0, 14.0)
12β	2.49, dt (18.0, 2.8)	2.29, dt (16.7, 2.9)	2.63, dt (18.0, 3.2)	2.05, br d (16.6)	2.65, dt (16.0, 4.2)
15	6.85, dd (17.2, 11.0)	6.57, dd (17.2, 11.0)	7.27, dd (17.2, 11.0)	3.62, dd (4.4, 2.7)	6.62, t (5.6)
16a	5.43, d (17.2)	5.25, d (17.2)	5.67, d (17.2)	2.88, dd (5.2, 4.4)	4.32, dd (15.2, 5.6)
16b	5.32, d (11.0)	5.13, d (11.0)	5.59, d (11.0)	2.73, dd (5.2, 2.7)	4.27, dd (15.2, 5.6)
17	8.33, s	5.30, br d (10.7)	10.19, s	8.11, s	—
Me-18	0.89, s	0.90, s	0.99, s	0.89, s	0.90, s
Me-19	0.87, s	0.88, s	0.84, s	0.87, s	0.88, s
Me-20	0.92, s	0.91, s	1.01, s	0.91, s	0.97, s

[a] δ 10.68 (1H, br s, OH) and 7.55 (1H, br s, OH). [b] δ 3.39 (1H, dd, *J* = 17.3, 10.7, H-21), 2.65 (1H, dd, *J* = 17.3, 2.4 Hz, H-21') and 2.21 (3H, s, Me-23). [c] δ 2.58 (1H, d, *J* = 3.5, OH). [d] δ 4.00 (1H, br s, OH).

Table 2. ^{13}C NMR Data for **2**–**6** in $CDCl_3$ at 100 MHz

	δ_C, type				
Carbon	**2**	**3**[a]	**4**	**5**	**6**
1	40.7, CH_2	40.7, CH_2	39.0, CH_2	40.7, CH_2	41.1, CH_2
2	18.8, CH_2	18.8, CH_2	18.7, CH_2	18.7, CH_2	18.8, CH_2
3	41.8, CH_2	41.9, CH_2	41.5, CH_2	41.8, CH_2	41.9, CH_2
4	34.5, C	34.6, C	39.0, C	34.6, C	34.6, C
5	47.5, CH	48.1, CH	52.7, CH	47.8, CH	47.9, CH
6	33.6, CH_2	33.2, CH_2	31.5, CH_2	31.9, CH_2	32.2, CH_2
7	97.6, CH	97.6, CH	176.0, C	96.3, CH	95.6, CH
8	67.2, CH	67.9, CH	72.1, CH	67.0, CH	74.6, CH
9	56.1, CH	56.3, CH	53.9, CH	55.5, CH	54.8, CH
10	38.7, C	38.7, C	39.3, C	39.0, C	39.9, C
11	21.2, CH_2	21.7, CH_2	21.5, CH_2	21.2, CH_2	22.0, CH_2
12	27.9, CH_2	26.5, CH_2	26.8, CH_2	21.2, CH_2	25.9, CH_2
13	145.3, C	136.1, C	155.5, C	127.3, C	136.8, C
14	128.5, C	133.8, C	132.6, C	146.0, C	200.5, C
15	132.7, CH	133.0, CH	130.8, CH	48.0, CH	136.9, CH
16	118.5, CH_2	115.4, CH_2	122.7, CH_2	45.5, CH_2	59.5, CH_2
17	146.9, CH	67.2, CH	189.2, CH	160.6, CH	—
18	33.3, Me	33.3, Me	33.4, Me	33.3, Me	33.5, Me
19	22.4, Me	22.4, Me	21.4, Me	22.4, Me	22.6, Me
20	15.3, Me	15.3, Me	14.1, Me	15.3, Me	15.6, Me

[a] δ 210.4 (C, C-22), 52.2 (CH_2, C-21) and 30.4 (Me, C-23).

In general, the new derivatives **2**–**6** did not overcome the cytotoxic activity of the natural product **1**, which, as mentioned above, possesses a γ,δ-unsaturated carbonyl system that appears to be important for its activity as an alkylating agent. Compounds **2**, **4**, and **6** preserve the double bond systems conjugated to an oxime or a carbonyl group, and could also act as Michael acceptors. The change of the carbonyl group at C-17 to an oxime group in **2**, as well as that of the hemiacetal group at C-7 to a lactone in **4**, do not have great influence on the antiproliferative activity. In addition, derivative **5**, instead having an unsaturated carbonyl system, possesses an epoxide group at C-15–C-16 and a formate group at C-14, a pair of electrophilic sites that could be responsible for its activity. It is also interesting that **3**, instead having the unsaturated carbonyl system has a β-hydroxyketone, it still presented activity comparable with that of the other derivatives. All of the above leads us to conclude that the *seco*-oxacassane diterpenoid hydrocarbon skeleton of compounds **1**–**6** is responsible for the important affinity for the active site, and then the secondary interactions as Michael or electrophilic acceptors, together with the conceivable hydrogen bonding interactions of the hemiacetal group, or the β-hydroxyketone, govern the antiproliferative activity exhibited by the compounds described herein.

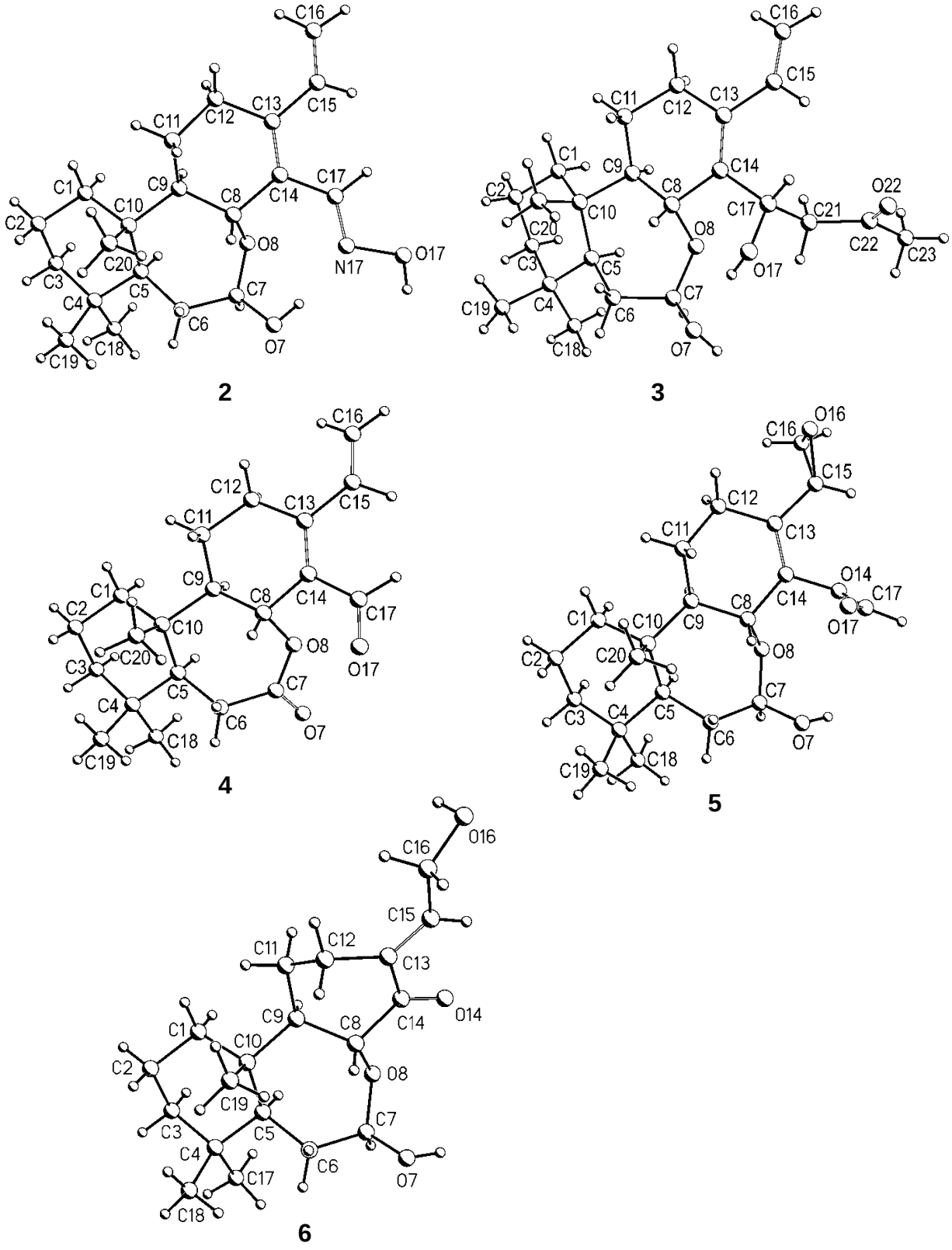

Figure 1. PLUTO plots of the single-crystal X-ray diffraction structures of **2**–**6**. The atom numbering for C-17, C-18, and C-19 in **6** differs from the usual *seco*-oxacassane atom numbering

Table 3. Crystal data, structure solution, and refinement parameters for **2–6**

	2	**3**	**4**	**5**	**6**
Formula	$C_{20}H_{31}NO_3$	$C_{23}H_{36}O_4$	$C_{20}H_{28}O_3$	$C_{20}H_{30}O_5$	$C_{19}H_{30}O_4$
Molecular weight	333.46	376.52	316.42	350.44	322.43
Crystal size (mm)	0.20 × 0.2 × 0.16	0.26 × 0.22 × 0.18	0.60 × 0.60 × 0.50	0.50 × 0.40 × 0.20	0.20 × 0.20 × 0.16
Crystal system	triclinic	orthorhombic	orthorhombic	monoclinic	monoclinic
space group	*P*1	$P2_1P2_1P2_1$	$P2_1P2_1P2_1$	$P2_1$	$P2_1$
a (Å)	8.5670(3)	7.6386(1)	9.870(2)	11.844(2)	9.6201(9)
b (Å)	9.8081(4)	11.0734(1)	11.916(2)	5.9245(8)	10.439(1)
c (Å)	12.1583(4)	25.6159(4)	14.919(3)	13.574(1)	18.171(2)
α (deg)	95.230(3)	90	90	90	90
β (deg)	101.649(3)	90	90	101.48(11)	101.569(9)
γ (deg)	105.770(3)	90	90	90	90
Volume ($Å^3$)	951.28(6)	2166.73(5)	1754.6(6)	933.4(2)	1787.8(3)
Z, ρ_{Calc} (mg/mm^3)	2, 1.164	4, 1.154	4, 1.198	2, 1.247	4, 1.198
μ (mm^{-1})	0.610	0.611	0.622	0.715	0.082
F(000)	364	824	688	380	704
θ range for data collection (deg)	3.76 to 78.50	3.45 to 77.62	4.75 to 74.48	3.32 to 77.95	2.97 to 29.63
Reflections collected / [R(int)]	32535 / 0.0390	36505 / 0.0283	21609 / 0.0263	4066 / 0.0307	20385 / 0.0531
Reflections unique	7557	4583	3592	2682	8514
Data / parameters	6681 / 472	4419 / 281	3539 / 232	2424 / 243	4438 / 439
Final R1, wR2 (%)	4.2, 11.6	4.3, 12.4	3.9, 10.8	4.8, 12.7	4.8, 8.5
Residual e^- ($e.Å^3$)	0.133	0.314	0.212	0.183	0.274
Flack and Hooft	0.08(8), 0.09(8)	−0.06(5), −0.06(4)	0.04(6), 0.07(4)	0.1(3), −0.1(2)	-
Inverted Flack and Hooft	0.92(8), 0.92(8)	1.06(5), 1.06(4)	0.96(6), 0.93(4)	0.9(3), 1.1(2)	-
CCDC number	2059548	2059550	2059558	2059566	2059567

In conclusion, it is evident that natural product **1** exhibits an abnormal reactivity behavior for oxidation reactions, particularly the resistance of the aldehyde group to be oxidized to the carboxylic acid. It is remarkable that the hemiacetal group at C-7 oxidizes to the corresponding lactone while the aldehyde group remains intact under Jones oxidation reaction conditions. Another interesting aspect is that the reactivity of the *γ*,*δ*-unsaturated carbonyl system towards nucleophilic additions is focused on the carbonyl group, since hydroxylamine, the enolate of acetone, and the peroxyacid are added to the carbonyl carbon. However, the *γ*,*δ*-unsaturated system plays an important role in the Baeyer-Villiger oxidation. Everything seems to indicate that the double bonds are electronically deficient to undergo an attack by the peroxyacid, so it is feasible that the formate group is generated first, and once this group is produced, the conjugated double bond system is available for epoxidation at C-15–C-16. This abnormal reactivity could play a capital role

for the chemical stability of the molecules in biological media, suggesting that their stability could be important for long term activity as the molecules are not so easily degraded while being in action. The important antiproliferative activity of the *seco*-oxacassanes **1**–**6** against the four explored cell lines suggests that they could generated a new and promissory class of anticancer agents.

Table 4. Antiproliferative activity (IC_{50} in μM) of **1**–**6**

Compd.	C2C12		L929		SiHa		MDA-MB-231	
	24 h	48 h	24 h	48 h	24 h	48 h	24 h	48 h
1	1.08±0.06	1.02±0.16	0.42±0.03	0.22±0.22	0.42±0.06	0.11±0.03	0.80±0.28	0.69±0.16
2	1.96±0.57	0.11±0.27	0.80±0.24	0.30±0.18	2.33±0.30	0.38±0.24	1.05±0.36	0.53±0.18
3	1.49±0.13	0.65±0.11	0.61±0.16	0.51±0.05	1.86±0.29	0.84±0.24	0.84±0.29	0.34±0.08
4	1.17±0.06	0.97±0.51	0.34±0.25	0.22±0.03	2.87±1.04	1.27±0.35	1.17±0.41	0.60±0.09
5	1.03±0.09	0.78±0.23	0.78±0.14	0.05±0.03	1.50±0.83	0.27±0.03	0.56±0.03	0.46±0.11
6	1.27±0.47	0.44±0.22	1.23±0.74	0.37±0.37	2.95±1.58	1.19±0.31	1.89±0.74	0.68±0.37
5-FU		—		2.98[a]				11.40[b]
Cisplatin		—				7.84[c]		19.13[c]

[a] Data from ref. 16, [b] ref. 17, [c] ref. 18.

EXPERIMENTAL

General experimental procedures. Melting points were determined on a Fisher-Johns melting point apparatus and are uncorrected. Optical rotations were determined in $CHCl_3$ solutions on a Perkin-Elmer 341 polarimeter. The IR spectra were recorded in the 4000–400 cm^{-1} region using KBr pellets on a Perkin Elmer 2000 FTIR spectrophotometer. The ^1H and ^{13}C NMR spectra, including gCOSY, gHSQC, and gHMBC experiments, were performed on a Bruker Ascend instrument at 400 MHz for ^1H and 100 MHz for ^{13}C from $CDCl_3$ solutions using the solvent residual proton signal centered at 7.26 ppm for ^1H and the central carbon signal at 77.2 ppm for ^{13}C. HRESIMS were determined on a Waters Synapt G2 spectrometer at the Department of Biochemistry, University of Colorado, Boulder, CO, USA. Column chromatographic separations were done using Merck silica gel 60 (Aldrich, 230–400 mesh ASTM).

Oxime 2. To a solution of **1** (300 mg) in EtOH (20 mL) was added hydroxylamine hydrochloride (199 mg) and sodium acetate (235 mg) in H_2O (2 mL). The mixture was stirred at room temperature for 1 h, diluted with water, and extracted with CH_2Cl_2. The organic layer was dried over Na_2SO_4, filtered, and evaporated to provide **2** (198 mg, 66%) as colorless prisms, mp 210–212 °C; $[\alpha]_D$ –177.0 (*c* 1.12, $CHCl_3$); IR ν_{max} 3471, 2900, 1631 cm^{-1}; ^1H and ^{13}C NMR, see Tables 1 and 2, respectively; HRESIMS: *m/z* 334.2375 $[M + H]^+$ (calculated for $C_{20}H_{31}NO_3 + H^+$, 334.2377).

***β*-Hydroxyketone 3.** A sample **1** (100 mg) in acetone (10 mL) was treated with a solution of NaOH (38 mg) in EtOH-H_2O (5:1, 6 mL). The mixture was stirred for 1 h at room temperature, neutralized with diluted H_2SO_4, extracted with EtOAc, washed with water, dried over Na_2SO_4, filtered, and evaporated affording **3** (49.5 mg, 42%) as colorless prisms, mp 174–176 °C; $[\alpha]_D$ +6.7 (*c* 0.5, $CHCl_3$); IR ν_{max} 3431, 3274, 2960, 1722, 1000 cm^{-1}; ^1H and ^{13}C NMR, see Tables 1 and 2, respectively; HRESIMS: *m/z* 399.2501 $[M + Na]^+$ (calculated for $C_{23}H_{36}O_4 + Na^+$, 399.2506).

Aldo-*ε*-lactone 4. A solution of **1** (250 mg) in acetone (20 mL) was treated with Jones reagent (CrO_3, 200 mg; H_2SO_4, 0.2 mL; H_2O, 1 mL) under stirring at 0 °C for 1 h. The reaction mixture was diluted with water and extracted with EtOAc. The organic layer was washed with a saturated aqueous solution of $NaHCO_3$, and water, dried over Na_2SO_4, filtered, and evaporated to give **4** (207 mg, 83%) as pale yellow prisms, mp 233–234 °C; $[\alpha]_D$ –107.7 (*c* 1.55, $CHCl_3$); IR ν_{max} 2980, 1742, 1672, 1250 cm^{-1}; ^1H and ^{13}C NMR, see Tables 1 and 2, respectively; HRESIMS: *m/z* 317.2120 $[M + H]^+$ (calculated for $C_{20}H_{28}O_3 + H^+$, 317.2111).

Epoxyformate 5. To a solution of **1** (300 mg) in CH_2Cl_2 (25 mL) was added *m*-chloroperbenzoic acid (325 mg). The mixture was refluxed for 2 h and evaporated to dryness. The residue, dissolved in *n*-hexanes–acetone (4:1), was filtered on a short silica gel column providing **5** (173 mg, 59%). Colorless prisms, mp 143–146 °C; $[\alpha]_D$ –52.1 (*c* 0.5, $CHCl_3$); IR ν_{max} 3514, 2990, 1690, 1170 cm^{-1}; ^1H and ^{13}C NMR, see Tables 1 and 2, respectively; HRESIMS: *m/z* 357.2249 $[M + Li]^+$ (calculated for $C_{20}H_{30}O_5 + Li^+$, 357.2248).

17-*nor*-Ketone 6. To a stirred solution of **5** (40 mg) in MeOH (5 mL) was added a solution of $NaHCO_3$ (20 mg) in H_2O (2 mL). The mixture was stirred for 15 min at room temperature, concentrated to a small volume under vacuum, and extracted with EtOAc. The organic layer was washed with water, dried over Na_2SO_4, filtered, and evaporated affording **6** (25 mg, 68%) as colorless prisms, mp 143–145 °C; $[\alpha]_D$ –34.0 (*c* 0.5, $CHCl_3$); IR ν_{max} 3370, 2944, 1712, 1150 cm^{-1}; ^1H and ^{13}C NMR, see Tables 1 and 2, respectively; HRESIMS: *m/z* 345.2034 $[M + Na]^+$ (calculated for $C_{19}H_{30}O_4 + Na^+$, 345.2036).

Single-crystal X-ray diffraction analysis

Data were collected using an Agilent Xcalibur Atlas Gemini diffractometer in the ω-2θ scan mode at room temperature. Crystals of **2**–**5** were measured with graphite-monochromated Cu *K*α radiation (λ = 1.54184 Å) while data of **6** followed from graphite-monochromated Mo *K*α (λ = 0.71073 Å) radiation. The structures were solved by direct methods using the Sir2004 software. All structure refinements were done by full–matrix least-squares on F^2 and the non-hydrogen atoms were treated anisotropically. Most hydrogen atoms, included in the structure factor calculation, were placed at idealized positions and refined isotropically,

while the labile hydrogen atoms were found in difference Fourier syntheses calculations. Relevant crystal data are given in Table 3. The data have been deposited with the Cambridge Crystallographic Data Centre from where they can be obtained, free of charge, via http://www.ccdc.cam.ac.uk/conts/retrieving.html. The CCDC deposition numbers are given in Table 3.

Cell line and culture conditions

Mouse myoblast C2C12 (CR-1772) cells, mouse fibroblast L929 (CCL-1) cells, cervix carcinoma SiHa (HTB-35) cells, and adenocarcinoma mammary gland MDA-MB-231 (HTB-26) cells were procured from the American Type Culture Collection (ATCC®, USA). The cell lines were cultured in a Dulbecco´s Modified Eagle Medium (DMEM), 10% fetal bovine serum, 1% L-glutamine and 1% penicillin-streptomycin. Cells were seeded in 25 cm^2 flasks until monolayer reached 70% confluence, then they were separated using trypsin and again seeded in 96 well plates to a confluence 1×10^4 cells/well added to 100 μL. All cell lines were cultured in a 5% CO_2 humidified atmosphere at 37 °C.

Cytotoxic activity and cell viability assays

The cells viability followed from the reduction of 3-(4,5-dimethylthiazol-2-yl)-2,5-diphenyltetrazolium bromide (MTT) to formazan. Exponentially growing C2C12, L929, SiHa, and MDA-MB-231 cells were seeded into 96-well plates at 1×10^4 cells/well in 100 μL. The culture medium was removed after 24 h. The cells were incubated in a 5% CO_2 atmosphere with 1×10^{-7}, 1×10^{-6}, 1×10^{-5}, 1×10^{-4}, 1×10^{-3}, 0.01, 0.1, and 1 μg/mL of **1**–**6** at 37 °C for 24 and 48 h. Cells incubated with dimethyl sulfoxide (DMSO) in a DMEM medium served as the positive control, while cells incubated in the culture medium served as the negative control. MTT (100 mg/0.1 mL phosphate buffered saline) was added to each well, the cells were incubated at 37 °C for 2 h, and DMSO (100 μL) was added to dissolve the formazan crystals. The absorbance was measured at 570 nm using an enzyme-linked immunosorbent assay (ELISA) plate reader. Cell viability was expressed as the percentage relative to controls and the IC_{50} is the concentration causing 50% cell death at a given time. The results of three independent experiments are shown.

ACKNOWLEDGEMENTS

Partial financial support from CONACYT, Mexico (Grants No. 238206 and 284194) is acknowledged. AHJ and RVA thanks CONACYT for fellowships No. 623150 and 453439.

REFERENCES

1. J. J. Manríquez-Torres, J. M. Torres-Valencia, M. A. Gómez-Hurtado, V. Motilva, S. García-Mauriño, J. Ávila, E. Talero, C. M. Cerda-García-Rojas, and P. Joseph-Nathan, *J. Nat. Prod.*, 2011, **74**, 1946.

2. D. J. Newman and G. M. Cragg, *J. Nat. Prod.*, 2020, **83**, 770.
3. D. Camp, A. Garavelas, and M. Campitelli, *J. Nat. Prod.*, 2015, **78**, 1370.
4. A. Talavera-Alemán, M. A. Gómez-Hurtado, G. Rodríguez-García, A. Ochoa-Zarzosa, C. Thomassigny, C. M. Cerda-García-Rojas, P. Joseph-Nathan, and R. E. del Río, *Heterocycles*, 2020, **100**, 207.
5. J. M. Torres-Valencia, V. Motilva, J. J. Manríquez-Torres, S. García-Mauriño, M. López-Lázaro, H. Zbakh, J. M. Calderón-Montaño, M. A. Gómez-Hurtado, J. A. Gayosso-De-Lucio, C. M. Cerda-García-Rojas, and P. Joseph-Nathan, *Nat. Prod. Commun.*, 2015, **10**, 853.
6. R. L. Shriner, R. C. Fuson, and D. Y. Curtin, 'Systematic Identification of Organic Compounds. A Laboratory Manual', Fifth Edition, John Wiley and Sons, New York, 1964, p. 173.
7. B. S. Bal, W. E. Childers Jr., and H. W. Pinnick, *Tetrahedron*, 1981, **37**, 2091.
8. S. Mannam and G. Sekar, *Tetrahedron Lett.*, 2008, **49**, 1083.
9. R. Mazitschek, M. Mülbaier, and A. Giannis, *Angew. Chem. Int. Ed.*, 2002, **41**, 4059.
10. D. Chakraborty, C. Majumder, and P. Malik, *Appl. Organomet. Chem.*, 2011, **25**, 487.
11. J. Meinwald, J. Crandall, and W. E. Hymans, *Org. Synth.*, 1965, **45**, 77.
12. C. H. Hassall, *Org. React.*, 2011, 73. DOI:10.1002/0471264180.or009.03/
13. H. D. Flack and G. Bernardinelli, *Chirality*, 2008, **20**, 681.
14. R. W. W. Hooft, L. H. Straver, and A. L. Spek, *J. Appl. Crystallogr.*, 2008, **41**, 96.
15. T. Mosmann, *J. Immunol. Methods*, 1983, **65**, 55.
16. X. Li, Z. Wu, L. Xu, C.-L. Chi, and B.-Q. Chen, *Med. Chem. Res.*, 2020, **29**, 180.
17. O. M. AboulWafa, H. M. G. Daabees, and W. A. Badawi, *Bioorg. Chem.*, 2020, **99**, 103798.
18. D. Stefkó, N. Kúsz, A. Csorba, G. Jakab, P. Bérdi, I. Zupkó, J. Hohmann, and A. Vasas, *Tetrahedron*, 2019, **75**, 116.